

以遺傳演算法鑑別結構接點參數 Identification of Structural Joint Parameters Using Genetic Algorithms

楊大中^{*1} 何信宗¹ 林崇賢²
Tachung Yang^{*1}, Shin-Tzung Ho¹, Chorng-Shyan Lin²

摘要

複雜結構是由許多結構透過接點來連接所組合而成，這些接點的動態特性影響結構機械動態性能。接點不易準確建模分析，接點參數鑑別程序在分析上相當複雜，易形成一病態數值系統，及受雜訊干擾。遺傳演算法來自於生物自然演化，對於搜索全域空間之最佳解有很好的成效，具有相當好的強健性。本文利用結構的頻率響應函數資訊與遺傳演算法，針對一單邊支撐樑之螺栓接點參數進行鑑別。首先，本文利用結構的自然頻率鑑別接點勁度參數，並且將鑑別結果與子結構合成法比較，再加入結構的振幅與相位資訊來鑑別接點阻尼參數。當使用的資訊越多時，鑑別的準確性有明顯提升。本文採取兩階段設定群體搜索範圍之方式以增進參數鑑別之精確度。

關鍵詞：接點鑑別，自然頻率，頻率響應函數，遺傳演算法

Abstract

Dynamic characteristics of complicated structures are greatly affected by various joints where the components are connected with each other. However, the joints are very difficult to model adequately and accurately. The parameter identification procedures of the joints are numerically complicated, ill-conditioned, and very sensitive to noise. Genetic Algorithm (GA), which imitates the evolution of nature, seems a very promising means in dealing with these identification problems. In this paper, the parameter identification procedure is carried out by implementing the Genetic Algorithm (GA), and using the Frequency Response Function (FRF) of the structure in the objective functions. First, the joint stiffness parameters of translation and rotation are identified using the natural frequency information and compared with those identified by substructure synthesis method. Damping parameters of the joint, then, are identified by using amplitudes and phase angles of FRFs. The identification of the joint parameters of a cantilever beam bolted at one end is conducted in this paper. The results show that the accuracy of identification increases if more FRFs information is used in the objective functions of the identification procedure. A two-stage strategy of defining search regions is used in this paper to promote the accuracy of the identified parameters.

Keywords: genetic algorithm, parameter identification, joint, frequency response function

I. INTRODUCTION

Generally, structures include various joints where the components are connected with each other. The joints have great influence on the static and dynamic characteristics of the structures, and they are also the most difficult parts of the structure to model for analysis purposes [1]. Therefore, accurate modeling of the joint characteristics appears to be critical to the dynamic analysis of structures.

Plenty of research works have been done on the parameter identification of joints. Kim et al. [2] pointed out

that the dynamic behaviors of structures can not be analyzed by FEM alone without knowing the joint characteristics. They utilized AMAV method (Autoregressive Moving Average Vector) to extract the modal data of the joint. Then, Riccati iteration algorithm is used to reduce the matrix order of the finite element models. Stiffness and damping of the joint are obtained using least squares method by comparing the modal results from FEM and modal experiment. Tsai and Chou [3] used the substructure synthesis method with FRFs to identify two types of bolt joints on

¹元智大學機械系 ²中山科學院第二研究所

^{*}Corresponding author. E-mail: mety@saturn.yzu.edu.tw

¹Department of Mechanical Engineering, Yuan Ze University, Chung Li, Taiwan, R.O.C.

²Chung-Shan Institute of Science and Technology, Lung-Tan, Taoyuan, Taiwan, R.O.C.

Manuscript received 26 June 2007; revised 12 September 2007; accepted 27 September 2007

overlapped beams. They used only the FRF data related to the joint and reduced the dimension of identification matrix, which in turn increases the efficiency of identification. Yang [4] applied techniques of weighting and sensitivity to improve the identification accuracy when the structure has too large or too small deformation in the joint in the frequency range.

Recently, more research results [5, 6] showed that the joint could be modeled by translational and rotational springs reasonably. Yang et al. [7] further investigated the cross coupling effect between the translational and rotational springs, and improved the accuracy of joint identification.

Genetic Algorithm (GA), proposed by Holland [8], is analogous to natural evolution and natural genetics. GA is very effective in search global optimum, simple to implement, and robust to noise. It is suitable to solve discontinuous problems, problems with noise interference, multidimensional problems, and polynomial problems.

Zimmerman and Yap [9] used GA and experimental modal data to modify finite element models. The optimization is solved by searching for the highest fitness of the FE model, which minimizes the natural frequency discrepancy between the finite element modeling and measurement. Zhang and Naghdy [10] identified the systems of SISO and MIMO, and nonlinear systems by using GA. Faster convergence and less information required are the advantages of GA over traditional optimization methods. Lin and Yang [6] successfully implemented GA to search for the joint parameters of a servomechanism with multiple joints. They found that design variables, which are more critical to the performance of the machine, will have less dispersion of identified values if the design variables have larger sensitivity with respect to the objective function, which is very helpful in the design of machinery.

In this paper, the identification of the joint parameters of a cantilever beam bolted at one end was conducted by using GA and FRF data of different modes. The identified results are compared with those identified by substructure synthesis method. Multiple parameters of the boundary conditions are identified, which greatly improves the simplified boundary models in the previous research [7]. The key parameters of the Genetic Algorithm, which influence the accuracy and efficiency of the procedure, are investigated.

II. THEORETICAL ASPECTS

1. GA identification procedure and settings

Genetic Algorithm is a numerical algorithm of random search that mimics natural evolution. It consists of the mechanisms of natural evolution, like reproduction, crossover, mutation, etc.. Through these evolution mechanisms, the global optimum solutions of design problems can be obtained. Srinivas and Patnaik [11] thought that GA can search larger design space than traditional optimization

methods and the performance of GA would depend on the selection of design variables, setting of crossover and mutation rates, and the convergence of design variables. The procedure of GA method can be illustrated by Fig. 1, and briefly introduced as follows [12]:

1-1. Initial population

If no previous experience exists for solving the engineering problems, it is difficult to define the search region of the possible solutions of design variables. If a larger search region is initially defined, computation time will be longer, although there is more variation for the individuals and less chance to be trapped in some local optimum solutions. However, if the initial search region is defined too small, either the global optimum can be excluded from the search region, or the convergence will be too speedy and the solution will be located in some local optimum.

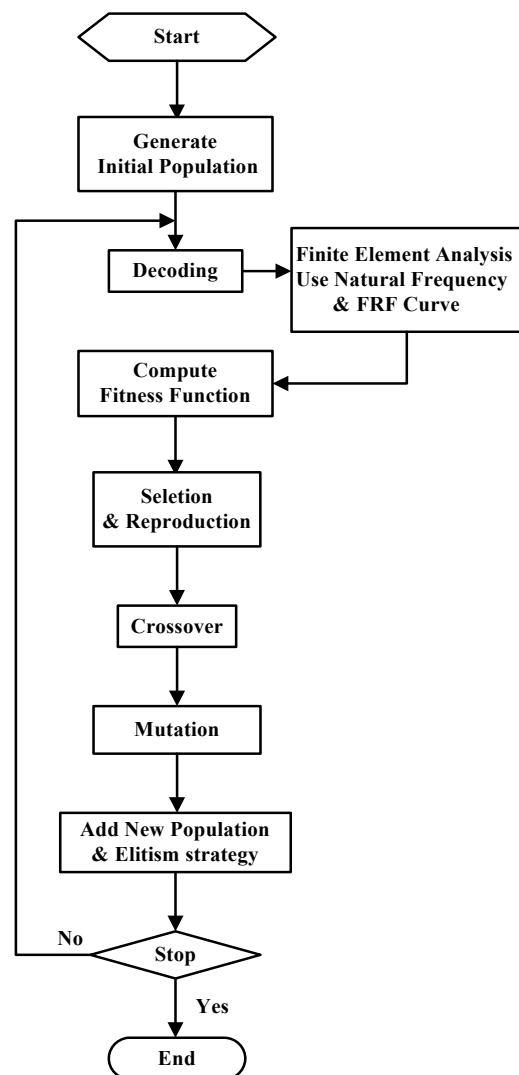


Fig. 1 Identification flow chart

In the determination of the search region, a two-stage strategy is used in this study. If the initially given search region of the design variables is too large, the resolution of the coding will be poor, the chance of finding the optimum solutions will diminished and the evolution time will be increased. A proper search region is critical to the accuracy and efficiency of the GA method. Therefore, A two-stage strategy of decoding is used in this paper to promote the accuracy of the results. At first, a larger search region of design variables is searched. The search region is reset as the dispersion region of design variables after 5 generations.

1-2. Coding

The requirement of coding for GA method is not stringent. Usually binary coding is used to simulate the gene of the chromosome. But in the design of the binary codes, two coding principles should be followed:

(1) Completeness.

All the desired solutions of design variables should be covered in the coding space of GA.

(2) Soundness and non-redundancy.

A one-to-one correlation between the GA coding string and the design variable must be ensured.

1-3. FEM analysis

In this work, a general-purposed FEM software is used to simulate the responses of the structures, and communicates with the GA identification program. The procedure is as following,

(1) Randomly generate the values of the joint parameters by the GA program.

(2) The GA program creates an input file for the FEM software, which includes the structural model and the joint parameters.

(3) The GA program issues an execution command to the FEM software and the FEM software starts simulation calculation.

(4) The GA program fetches the outputs of the FEM software, which contain the information of natural frequency, phase, and amplitude.

(5) The GA program evaluates the objective functions and executes the related procedures.

1-4. Fitness function.

Fitness means the probability of offsprings that the population undergoes reproduction, crossover, and mutation under the influence of environment. The relationship between fitness function and objective function can be expressed as [13] :

$$F_t = c - U(x) - r_p \left[\sum_{i=1}^p h_i^2 + \sum_{j=1}^m (g_j^+)^2 \right] \quad (1)$$

where F_t is fitness function; c a constant to ensure the value of fitness to be positive; U objective function; r_p penalty parameter; h_i equal constraints; g_j^+ unequal

constraints. The engineering problem in this work has no constraints, so the objective function is the only one to affect the fitness. Minimization of the objective function is equivalent to find the highest fitness.

1-5. Reproduction and selection

Whether an individual can be reproduced or eliminated is determined by fitness evaluation. The individuals with higher fitness values have larger chance to be selected into the crossover pool. The common selection methods are tournament selection and roulette wheel selection [12]. Tournament selection is adopted in this work. Two or more individuals are selected and comparison of fitness values is made. The individual with highest fitness value is kept and put into the crossover pool. The tournament selection is simpler in programming and has faster convergent rate as compared with the roulette wheel selection.

1-6. Crossover

Two individuals in the crossover are selected and exchange parts of their coding strings. Offsprings with higher fitness values are expected to generate. The common crossover rate, P_c , is between 0.6 and 1. Various types of crossover include single point crossover, double point crossover, multiple point crossover, and mask crossover. Double point crossover is used in this paper to avoid end-point effect.

1-7. Mutation

Switch a certain binary bit between 0 and 1 in order to generate possible individuals with higher fitness values, which have not yet appeared in the population. Usually the mutation rate is set between 0.005~0.01.

1-8. Adding new population and elitism strategy [12]

In this study, 5 individuals are randomly generated and added to the population to increase its diversity and to avoid premature convergence to local optimum. Furthermore, elitism strategy is applied. The best individual of each generation is preserved unconditionally to the next generation to avoid accidental loss of the best individual during evolution operations of crossover and mutation.

1-9. Stop criteria

Various stop criteria can be used based on different situations, e.g., maximum number of generations, convergence of the parameters, convergence of the objective functions, etc.. Since the convergent tolerance and the form of convergence evaluation are case-dependent, the criteria of maximum number of generations is used in this study to ensure the accuracy of the results and to simplify the programming, although some computation time is wasted.

2. Equations for joint parameters

The dynamic equations for the structure containing a joint, depicted in Fig. 2, can be presented as

$$[M]\{\ddot{q}\} + ([C] + [C_J])\{\dot{q}\} + ([K] + [K_J])\{q\} = \{f\} \quad (2)$$

where $\{q\}$ and $\{f\}$ are the displacement and external

loading vectors respectively. $[M]$, $[C]$, $[K]$ are the inertia, damping and stiffness matrices of the free-free beam. $[K_J]$ and $[C_J]$ are the stiffness and damping matrices for the joint, and can be in the forms of

$$[K_J] = \begin{bmatrix} K_t & K_{tr} \\ K_{rt} & K_r \end{bmatrix} \quad (3)$$

$$[C_J] = \begin{bmatrix} C_t & C_{tr} \\ C_{rt} & C_r \end{bmatrix} \quad (4)$$

In Eqs. (3) and (4), K_t is the translational stiffness, K_r rotational stiffness, C_t translational damping, C_r rotational damping. The cross coupling effects in the joint have not been investigated in this paper, so the cross coupling terms K_{tr} , K_{rt} , C_{tr} , C_{rt} are assumed to be zero.

Assuming the external loading is of harmonic excitation, so

$$\{f\} = \{f_0\} e^{j\omega t} \quad (5)$$

$$\{q\} = \{q_0\} e^{j\omega t} \quad (6)$$

Substitute Eqs. (5) and (6) into Eq. (2) and obtain

$$[H(\omega)] = \{([K] + [K_J]) + j\omega([C] + [C_J]) - (\omega^2[M])\}^{-1} \quad (7)$$

where $[H]$ is the matrix of Frequency Response Function (FRF).

For the objective function, we may compare the results of $[H]$ from analysis and experiment, and try to minimize the their errors. The objective function can be

$$U = \left(\sum_{i=1}^n w_i \left(\frac{y_i^F - y_i^E}{y_i^E} \right)^2 + \sum_{j=1}^m w_m \left(\frac{f_j^F - f_j^E}{f_j^E} \right)^2 + \sum_{k=1}^l w_k \left(\frac{p_k^F - p_k^E}{p_k^E} \right)^2 \right)^{1/2} \quad (8)$$

where y_i and p_k are the amplitude and phase for some selected frequencies in a certain resonant region, and f_j is the resonant frequency. Superscripts F and E denote the results from FEM analysis and experiment, respectively.

III. RESULTS AND DISCUSSION

The experimental set-up of the structure is shown in Fig. 3. A beam is bolted on an optical table to isolate other vibrations. A washer and two O-ring (6x3 NBR 70), to increase the damping effects, are inserted between the bolt

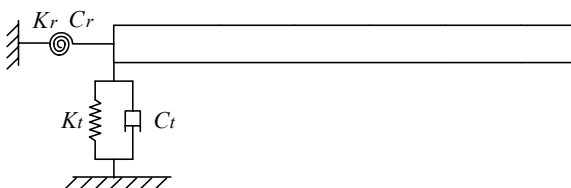


Fig. 2 Schematic diagram of the beam with one-end support

head and beam, and between the beam and the nut, separately. The torque applied is 0.982N-m (10 kgf-cm). In the FEM analysis, the beam is considered connected by a joint, modeled as $[K_J]$ and $[C_J]$, at one end, while free at the other end. The finite element modeling of the beam is presented in Fig. 4, its dimensions and material properties are listed in Table 1.

The operational factors of the GA program set for this work are population=40; 40 generations; crossover rate, $P_c=0.7$; mutation rate, $P_m=0.005$; double point crossover.

Four cases are studied in this paper, three simulation cases and one experimental case. Known target values of joint parameters are input into FEM simulation and the resultant data of natural frequency, phase, and amplitude are obtained. The simulation results are input into the GA identification program and the identified values of the joint parameters are compared with the target values of the joint parameters to validate the effectiveness and precision of the proposed procedure. Finally, The experimental data are input into the GA identification program to obtain the joint parameter for a real joint.

No damping is considered in case 1, so only two joint parameters, K_t and K_r , are to be identified. The objective function used is

$$U_1 = \left(\sum_{j=1}^{10} w_j \left(\frac{f_j^F - f_j^A}{f_j^A} \right)^2 \right)^{1/2} \quad (9)$$

The superscript A in Eq. (9) denotes the data of analysis, which are obtained from a separate FEM analysis for the beam with known joint parameters. Subscript $j=1$ to 10 means 10 natural frequencies are used. The identified values of the joint are shown in Table 2. The results from GA and substructural synthesis method [7] are very close to the target values of joint parameters for 4 different sets

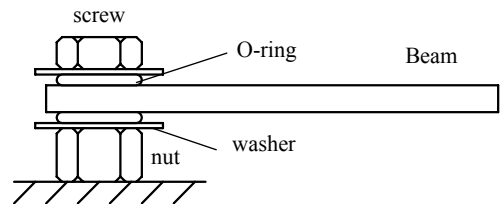


Fig. 3 Beam-support structure

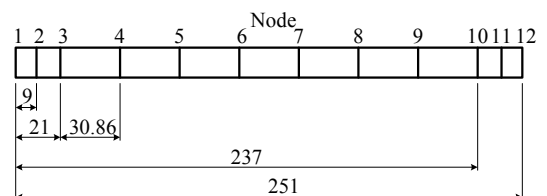


Fig. 4 Finite element modeling of the beam (mm)

Table 1 Dimensions and material properties of the beam

Dimension (mm)		
h	w	L
2.06	35.03	251
Material properties		
E	density (kg/m ³)	poisson
69.35GPa	2687.85	0.33

Table 2 Identified values of stiffness (Case 1)

parameter	preset value	substructure synthesis method	GA
1	Kt (N/m)	1E4	1001.7 (0.17%)
	Kr (N-m)	100	99.99 (-0.0002%)
2	Kt (N/m)	1E5	10000.14 (0.0014%)
	Kr (N-m)	1000	999.85 (-0.014%)
3	Kt (N/m)	1E6	100004.79 (0.0047%)
	Kr (N-m)	1E4	9970.17 (-0.298%)
4	Kt (N/m)	1E7	999928.59 (-0.0071%)
	Kr (N-m)	1E5	96413.58 (-3.586%)

of target values. However, when the target values of joints become larger, the results from GA still maintain at satisfactory levels, while accuracy of substructural synthesis method become worse. For example, in Table 2, when K_r is preset to be 1E5, the error of GA is 0.275%, while the error of substructural synthesis method is 3.6%.

Substructural synthesis method uses FRF data and matrix operation to solve for the joint parameters. So for a problem with n unknown joint parameters, at least $(n^2 + n)/2$ FRF curves (due to matrix symmetry) are needed to solve for the joint parameters at each frequency. However, GA method needs at least n sets of FRF data for each frequency, or n different set of data on the same FRF curve if the joint parameters are not frequency dependent. In addition, the accuracy of substructural synthesis method becomes degraded for the parameters of less sensitivity, e.g., K_r , while GA method still provide enough accuracy for those parameters.

Case 2 is to identify the joint damping parameters, C_t and C_r , with fixed joint stiffness parameters, $K_t = 4000\text{N/m}$ and $K_r = 500\text{N-m}$. Data of natural frequency, phase and amplitude are selected for a certain mode and within the resonant region of that mode. The objective function used is

$$U_2 = \left(\sum_{i=1}^n w_i \left(\frac{y_i^F - y_i^A}{y_i^A} \right)^2 + \sum_{j=1}^m w_j \left(\frac{f_j^F - f_j^A}{f_j^A} \right)^2 + \sum_{k=1}^l w_k \left(\frac{p_k^F - p_k^A}{p_k^A} \right)^2 \right)^{1/2} \quad (10)$$

In Table 3, the identified results are the mean values of the identified results from 5 runs. Accuracy of C_t seems better than that of C_r , due to the fact that more apparent motions in translation reveal in the mode shapes than rotation. In Fig. 5, the dispersion region of C_t for mode 2 seems wider than those for the other modes. The reason is that the joint end of the beam has less motion in mode 2 than in other modes. Same trend appear in Fig. 6 for C_r . The dispersion of the identified results converges and will be closer to the target values if more information is used in the GA identification, as illustrated in Fig. 6 for C_r when all data of 3 modes are used together. The corresponding FRF curves for identified parameters from mode 2, 3, 4, and all modes are very close to the FRF curve by using the target joint values, as compared in Fig. 7.

Case 3 is to identify the 4 joint parameters, K_t , K_r , C_t , C_r , simultaneously. Based on the experience of case 2, data of all modes are used. The objective function is

$$U_3 = \left(\sum_{i=1}^3 w_i \left(\frac{y_i^F - y_i^A}{y_i^A} \right)^2 + \sum_{j=1}^3 w_j \left(\frac{f_j^F - f_j^A}{f_j^A} \right)^2 + \sum_{k=1}^3 w_k \left(\frac{p_k^F - p_k^A}{p_k^A} \right)^2 \right)^{1/2} \quad (11)$$

Listed in Table 4 are the means and standard deviations of the identified results from 5 runs and the dispersion regions. In the dispersion regions of the identified results, C_t has the smallest region, that is because it has the

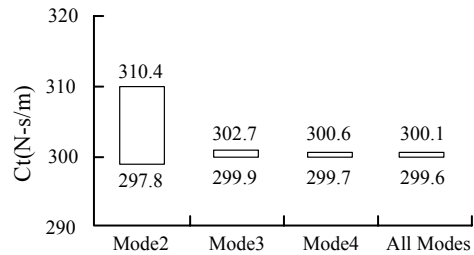


Fig. 5 Dispersion of the identified values C_t for each mode

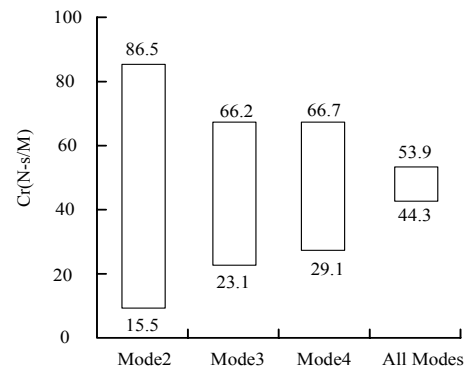


Fig. 6 Dispersion of the identified values C_r for each mode

Table 3 Identified values of damping (Case 2)
(preset values: $C_t=300, C_r=50$)

	mean	
	Ct (N-s/m)	Cr (N-m-s)
Mode 2	301.24 (0.41%)	57.54 (15.09%)
Mode 3	300.99 (0.33%)	57.20 (14.41%)
Mode4	300.26 (0.09%)	43.51 (-12.97%)
ALL Modes	300.05 (0.02%)	48.81 (-2.36%)

Table 4 Identified values of stiffness and damping (Case 3)
(preset values: $K_t=4000, K_r=500, C_t=300, C_r=50$)

parameter	mean	standard deviation	dispersion
Kt (N/m)	3994.69 (-0.13%)	325.14	$(4.014 \leq x \leq 4.49) \times 10^3$
Kr (N-m)	502.03 (0.41%)	50.22	$466.3 \leq x \leq 594.8$
Ct (N-s/m)	300.44 (0.15%)	0.237	$300.1 \leq x \leq 300.6$
Cr (N-m-s)	49.67 (-0.65%)	2.489	$47.6 \leq x \leq 53.5$

largest sensitivity in the designed objective function; whereas K_r has the largest dispersion region and the least sensitivity in this case. However, the FRF curves using the identified values in the dispersion region for 4 parameters will obtain satisfied results, as shown in Fig. 7 (curve 4-param).

Joint parameter identification by using the experimental data is shown in case 4, based on the same procedure of case 3. The operational factors of GA program are set as population=40; 40 generations, crossover rate; $P_c=0.7$; mutation rate; $P_m=0.005$; double point crossover. The objective function is

$$U_4 = \left(\sum_{i=1}^3 w_i \left(\frac{y_i^F - y_i^E}{y_i^E} \right)^2 + \sum_{j=1}^3 w_j \left(\frac{f_j^F - f_j^E}{f_j^E} \right)^2 + \sum_{k=1}^3 w_k \left(\frac{p_k^F - p_k^E}{p_k^E} \right)^2 \right)^{1/2} \quad (12)$$

where superscript E denotes experimental values. The means and standard deviations of the identified results from 5 runs and the dispersion regions are listed in Table 5. C_t has the largest sensitivity and K_r has the least sensitivity for this joint. The corresponding FRF curves using the mean values of 4 joint parameters are plotted in Fig. 8 and compared with the experimental FRF curves. The agreement is very satisfactory, which validates the effectiveness and precision of this GA identification program.

The convergence of the objective functions for the first 3 cases are shown in Fig. 9 and the objective function

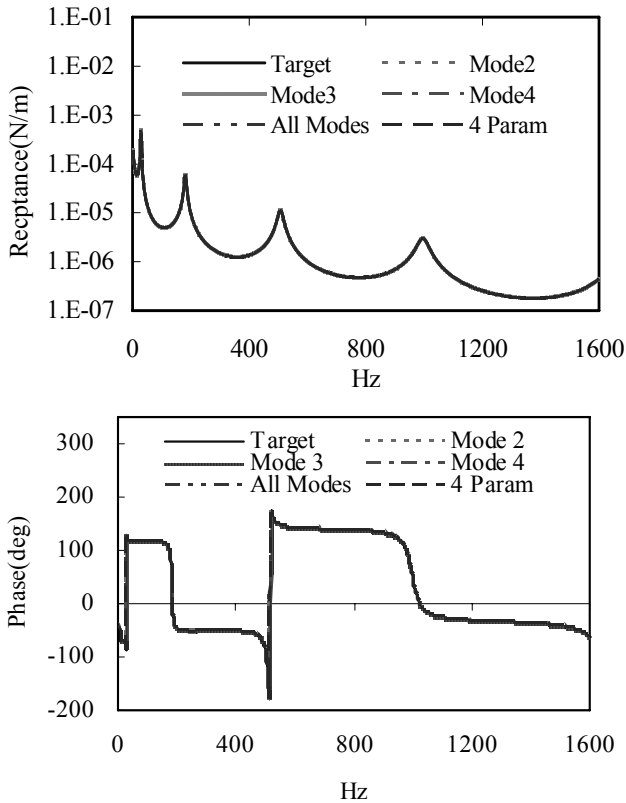


Fig. 7 Comparison of FRFs for H_{10_3} , FEM and GA simulation for preset boundary conditions

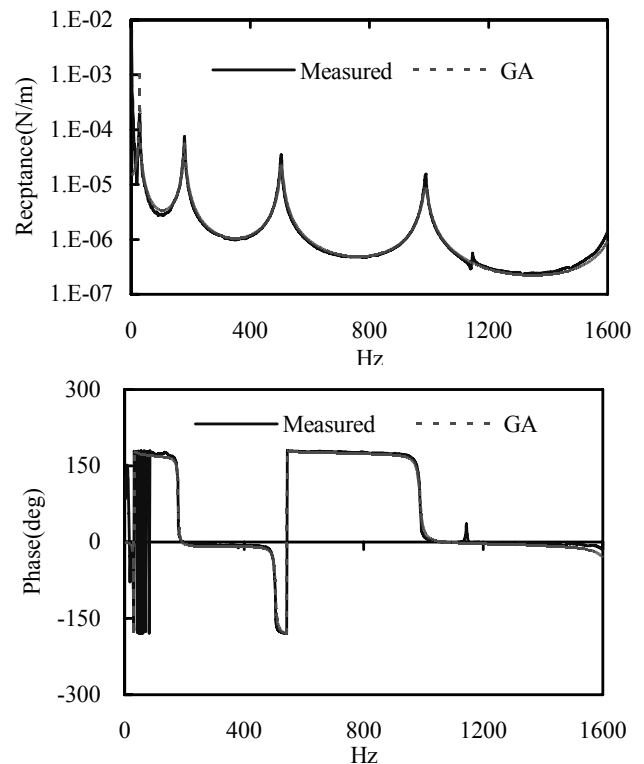


Fig. 8 Comparison of FRFs for H_{10_3} , measurement and simulation

Table 5 Identified results from test data (Case 4)

parameter	mean	Standard deviation	dispersion
Kt (N/m)	5300735.5	141094.8	$(5.2 \leq x \leq 5.5) \times 10^6$
Kr (N-m)	524.55	21.85	$501.17 \leq x \leq 552.02$
Ct (N-s/m)	150.45	0.298	$150.15 \leq x \leq 150.89$
Cr (N-m-s)	0.69	0.02	$0.638 \leq x \leq 0.72$

of case 4 is shown in Fig. 10. In Fig. 9, the objective functions converge after 10 generations; while in Fig. 10, the objective function converges after 15 generations. Also, the converged values of the objective functions in Fig. 9 are closer to zero than those in Fig. 10. The first 3 cases are numerical simulations and contain very little noise. In the contrast, data of case 4 are from experimental measurement and contain much noise. Therefore, convergence is slower in case 4.

IV. CONCLUSIONS

The Genetic Algorithm (GA) is applied to the joint parameter identification of structures in this paper. From the results of experiment and simulation, the following conclusions can be obtained:

1. When the values of the joint parameters become larger, accuracy of substructural synthesis method become worse, while the accuracy of GA still maintain at satisfactory levels, which is an advantage of GA.
2. Much less information is needed for GA to identify joint parameters, as compared with substructural synthesis method. Besides, there is more flexibility in the selection of the data needed for the GA, due to the design variety of the objective function of GA.
3. More accurate values of joint parameters can be obtained if more information is used in the objective functions of the identification processes. Also, the dispersion regions of the identified results will be reduced and closer to the target values.
4. The accuracy and dispersion of the identified results of joint parameters by using GA are dependent on the sensitivities of the parameters and the design of the objective functions.
5. The resolution of the identification results, which is determined by the search region and the length of coding strings, will affect the accuracy and efficiency of the identification process. A two-stage strategy of defining search regions is used in this paper to promote the accuracy of the results.

REFERENCES

- [1] Y. Ren and C. F. Beards, "On the importance of weighting for FRF joint identification," in *11th IMAC*, Florida, USA, pp. 1606-1611, 1993.
- [2] T. R. Kim, K. F. Ehmann and S. M. Wu, "Identification of joint structural parameters between substructures," *Journal of Engineering for Industry*, vol. 113, pp. 419-424, 1991.
- [3] Y. F. Chou and J. S. Tsai, "The identification of dynamics characteristics of a single bolt joint," *Journal of Sound and Vibration*, vol. 125, no. 3, pp. 487-502, 1988.
- [4] M. J. Yang, *The development of the method of the dynamic parameters identification of the mechanical joints*, MS Thesis, Department of Mechanical Engineering, National Tsing Hua University, Taiwan, 1996. (in Chinese)
- [5] D. B. Barker and Y. S. Chen, "Modeling the vibration restraints of wedge lock card guides," *ASME Journal of Electronic Packaging*, vol. 115, pp. 189-194, 1993.
- [6] C. S. Lin and T. Yang, "Joint parameters identification for a flexible servo- mechanism by using genetic algorithm," in *2002 Chinese Automatic Control Conference*, Tainan, Taiwan, pp. 1036-1041, 2002. (in Chinese)
- [7] T. Yang, S. H. Fan and C. S. Lin, "Joint stiffness identification using FRF measurements," *Computers and Structures*, vol. 81, no. 28-29, pp. 2549-2556, 2003.
- [8] J. H. Holland, *Adaptation in natural and artificial system*, Ann Arbor, Michigan, University of Michigan Press, 1975.
- [9] D. C. Zimmerman and K. Yap, "Evolutionary approach for model refinement," *Mechanical Systems and Signal Processing*, vol. 13, no. 4, pp. 606-625, 1999.
- [10] Z. Zhang and F. Naghdy, "Application of genetic algorithms to system identification," in *IEEE International Conference on Evolutionary Computation*, vol. 2, pp. 777-782, 1995.
- [11] M. Srinivas and L. M. Patnaik, "Genetic algorithms: a survey," *Computer*, vol. 27, pp. 17-26, 1994.
- [12] D. E. Goldberg, *Genetic algorithms in search, optimization, and machine learning*, Addison Wesley Publishing Company, Inc., 1989.
- [13] C. H. Chien, *A simple modeling method for bolted joints and its identification*, Master Thesis, Department of Mechanical Engineering, National Chung Hsing University, Taiwan, 2002. (in Chinese)

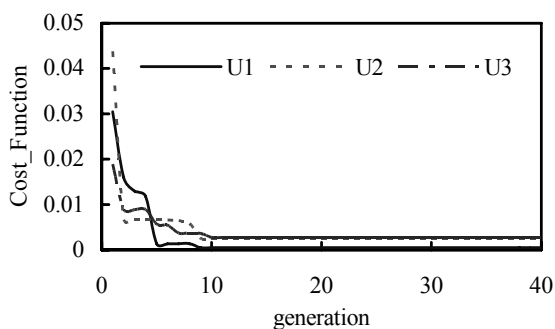


Fig. 9 Convergence of objective functions, U_1 , U_2 , and U_3

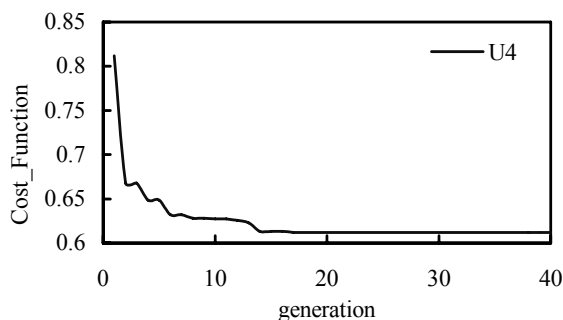


Fig. 10 Convergence of objective function, U_4